

Sustained Delivery of VEGF Maintains Innervation and Promotes Reperfusion in Ischemic Skeletal Muscles Via NGF/GDNF Signaling

Dmitry Shvartsman^{1,2}, Hannah Storrie-White¹, Kangwon Lee^{1,2}, Cathal Kearney¹, Yevgeny Brudno^{1,2}, Nhi Ho¹, Christine Cezar¹, Corey McCann³, Erin Anderson^{1,2}, John Koullias¹, Juan Carlos Tapia³, Herman Vandenburgh⁴, Jeff W Lichtman³ and David J Mooney^{1,2}

¹School of Engineering and Applied Sciences, Harvard University, Cambridge, Massachusetts, USA; ²Wyss Institute for Biologically Inspired Engineering, Cambridge, Massachusetts, USA; ³Department of Molecular and Cellular Biology, Harvard University, Cambridge, Massachusetts, USA; ⁴Department of Pathology, Brown Medical School–Miriam Hospital, Providence, Rhode Island, USA

Tissue reinnervation following trauma, disease, or transplantation often presents a significant challenge. Here, we show that the delivery of vascular endothelial growth factor (VEGF) from alginate hydrogels ameliorates loss of skeletal muscle innervation after ischemic injury by promoting both maintenance and regrowth of damaged axons in mice. Nerve growth factor (NGF) and glial-derived neurotrophic factor (GDNF) mediated VEGF-induced axonal regeneration, and the expression of both is induced by VEGF presentation. Using both *in vitro* and *in vivo* modeling approaches, we demonstrate that the activity of NGF and GDNF regulates VEGF-driven angiogenesis, controlling endothelial cell sprouting and blood vessel maturation. Altogether, these studies produce evidence of new mechanisms of VEGF action, further broaden the understanding of the roles of NGF and GDNF in angiogenesis and axonal regeneration, and suggest approaches to improve axonal and ischemic tissue repair therapies.

Received 25 February 2014; accepted 17 April 2014; advance online publication 20 May 2014. doi:10.1038/mt.2014.76

INTRODUCTION

Severe neuropathies result from traumatic injuries or the sudden loss of tissue perfusion (e.g., ischemic stroke). Unlike the central nervous system, regeneration is possible in the mammalian peripheral nervous system as peripheral axons can grow through vacant Schwann cell tubes.¹ However, trauma and neuropathic² diseases lead to loss of motor and sensory responses, and reinnervation is often neither robust nor precise. Current treatment options include direct surgical reinnervation with autologous nerve grafting, but these procedures typically do not achieve complete regeneration of the damaged nerve.³ Cues that encourage faster reinnervation following injury may provide new treatment options for peripheral nervous system disorders and provide mechanistic insights into neural regeneration; this is likely to also have applications in the central nervous system repair.⁴

Vascular endothelial growth factor (VEGF) has been identified in recent years as a potential component of therapeutic approaches aimed at restoring neural functions in damaged tissues.⁵ Initially, VEGF was recognized as one of the key factors in angiogenesis regulation,⁵ due to its ability to promote endothelial cell sprouting and blood vessel branching during fetal development, cancer malignancies, and wound healing in adult tissues. However, the similar anatomical patterns exhibited by the vascular and neural networks led to the identification of VEGF as a signaling factor facilitating the crosstalk between the neural and vascular systems.⁵ VEGF is expressed by multiple neuronal cell types and directly induces angiogenesis, which enhances tissue perfusion.⁵ VEGF also stimulates neurons and glial cells directly.⁵ During early developmental stages, tissue hypoxia upregulates VEGF expression and its gradient guides tissue innervation by the migrating axons.⁵ Signaling by VEGF also affects nervous system regeneration by modulating the local vasculature in damaged tissues.⁶ Under ischemic conditions, VEGF released from hypoxic endothelial cells directly stimulates proliferation of neural progenitor cells and provides neuroprotection of adult neurons in the peripheral nervous system.⁷ Several studies have shown the positive effects of delivery of exogenous VEGF, using either bolus injections of the recombinant protein or gene therapy approaches, to prevent neuronal degeneration and loss of innervation in several models of neurological disorders.⁸ These models included direct ligation or ischemic injury of the peripheral sciatic nerves, spinal cord damage, ischemic brain stroke, and neurodegenerative diseases such as amyotrophic lateral sclerosis and Parkinson's disease.⁸ VEGF protein delivery may have immediate clinical relevancy in human facial and limb transplantations, where there is the requirement for the restoration of functional innervation and sensory networks.⁹ However, approaches utilized for VEGF administration typically had limited success, likely due to the rapid clearance of VEGF protein delivered in solution form.¹⁰ Infusion of VEGF in clinical trials resulted in elevated VEGF plasma levels during the infusion, but this was followed by a rapid clearance of VEGF once infusions were discontinued, and undetectable levels

Correspondence: David J Mooney, School of Engineering and Applied Sciences, Harvard University, Cambridge, Massachusetts, USA. E-mail: mooneyd@seas.harvard.edu

resulted within 4 hours.¹⁰ The delivery of high doses was pursued in an effort to achieve therapeutic benefit with this approach to VEGF delivery, increasing the risks of malignant malformations, brain edema, ophthalmic injuries, and disruption of blood–brain barrier integrity.¹¹

The current study examined the effects of sustained local presentation of exogenous VEGF on neural axon survival in ischemic skeletal muscles. Polymeric hydrogels formed from alginate were used to deliver VEGF in a sustained and localized manner¹² following ischemic nerve injury in skeletal muscle. We have previously demonstrated that angiogenic sprouting is optimized with an early, high concentration of VEGF, followed by a lower, maintenance concentration.¹² The release kinetics of the hydrogel used in this manuscript was designed to yield this form of release kinetics.¹² One-time local delivery of VEGF (3 μg) with these alginate hydrogels into murine ischemic hindlimbs resulted in a prolonged presence (15–25 days) of the delivered VEGF in the surrounding muscle tissue.¹³ Importantly, presentation of VEGF was largely limited to the ischemic muscle, with little of the delivered VEGF detected in blood. We have previously demonstrated that bolus delivery of the same quantity of VEGF as encapsulated in these gels leads to rapid clearance from the tissue and no significant biological response.^{12,14} To evaluate axon survival and regeneration, either VEGF-containing or blank hydrogels were delivered to ischemic muscle in transgenic animals whose motor neurons express yellow fluorescent protein (YFP), which allows for direct observation of axons¹⁵ in normal mice. Notably, a new signaling mechanisms regulating neuronal survival, regeneration, and revascularization in skeletal muscles were observed, where GDNF and nerve growth factor (NGF) expression is upregulated during the initial stages of ischemic insult and with exogenous VEGF exposure.

RESULTS

Gel delivery of exogenous VEGF slows neural degeneration and enhances neural regrowth in ischemic skeletal muscle

To determine if exogenous VEGF would impact neural survival and reinnervation in the context of ischemic nerve injury, an alginate–hydrogel delivery system¹² was used to provide a localized and sustained release of VEGF in injured sternomastoid muscle nerve. Previously, we have demonstrated the validity of alginate hydrogels for localized delivery and prolonged presentation of active protein cargos *in vivo*, including VEGF.^{13,16} *In vitro*, recombinant VEGF was released from these gels with an initial burst over the first day, followed by a sustained release for over 25 days, in a similar manner for all VEGF doses (Figure 1a). A sternomastoid injury model was chosen due to its accessibility for time-lapse imaging and high levels of innervation.¹⁷ Motor end-plate innervation in the sternomastoid muscle of thy1-YFP line 16 (YFP-16) mice was examined upon induction of ischemia and neural crush, with and without gel-VEGF delivery (Figure 1b–d). As expected, the innervation of motor axon terminals in muscles was lost a day after the ischemic procedure. A VEGF dose of either 3 or 0.3 μg VEGF, however, resulted in partial and equivalent motor end-plate innervation at 24 hours (Figure 1b,c). No innervation was observed with hydrogels containing 0.03 μg VEGF (Figure 1d).

Untreated mice with injured sternomastoid muscle also demonstrated no innervation and characteristic Wallerian neural degeneration of the motor axons (Figure 1e). To investigate whether the neuromuscular innervation at 18 and 24 hours with VEGF delivery was caused either by the attenuation of degeneration following nerve crush, or rather by more rapid reinnervation, *in situ* time-lapse imaging was utilized to examine neuromuscular junctions (NMJ) in injured muscles. Axonal maintenance was only observed in muscles treated with VEGF-containing hydrogels, and the end plates that were occupied at 24 hours were innervated by the same axon at 4 and 12 hours (Figure 1f), indicating that axon maintenance, and not regeneration is responsible for the innervation observed at this time point after injury. Quantification of innervation revealed that the maintenance effect of exogenous VEGF gradually decreased, consistent with the time-lapse study, while blank gel delivery led to complete degradation at 24 hours (Figure 1g). This finding suggests that sustained VEGF delivery acts by slowing axonal degradation in the acute phase following nerve crush and ischemic insult. Both blank gel- and VEGF-gel-treated muscles rapidly recovered innervation after 24 hours in this injury model (Figure 1g). Delayed Wallerian degeneration following axotomy had previously been observed in the Wld^s mouse,¹⁸ however, VEGF was not implicated in those pathways responsible for axon maintenance. Under ischemic conditions, VEGF had been shown to provide neuroprotection of adult neurons and can also stimulate neural progenitor cells.⁷ This ability of VEGF to maintain synapses that would otherwise be lost due to changes at the motor end plates, which also may occur in neurodegeneration and as a result of aging,¹⁹ may have therapeutic implications.

The effects of gel-VEGF delivery on NMJ remodeling were next studied. Newly reinnervated NMJs that are multiply innervated or show terminal sprouting are characteristic of the immature NMJs occurring during early developmental stages, or at the sites of neural injury or degeneration.²⁰ In muscles treated with blank hydrogels (Figure 1h,i), multiple innervation (indicated by white arrow in Figure 1i) was initially observed to increase from day 3 to 6 and then to decrease at day 21 (Figure 1j). Terminal sprouts, identified as fine, neuritic processes bypassing the motor end-plate site (white arrow in Figure 1h), were also present on a majority of muscle end plates at day 3, and slowly decreased over the course of 3 weeks (Figure 1m). These data indicate that this ischemic injury leads to the reformation of immature NMJs that remodel slowly. Upon treatment with VEGF-containing hydrogels, however, less terminal axon sprouting was observed at motor end plates at all time points (Figure 1j,m), and no terminal sprouts remained at day 21. The percentage of end plates with multiple innervations in the VEGF group was similar to control muscles at day 3, but by day 7, multiple innervations was significantly less with VEGF than in muscles treated with blank hydrogels (Figure 1k,l). Altogether, these results indicate hydrogel-based delivery of exogenous VEGF attenuates acute axon degradation and promotes motor end-plate remodeling after injury. The accelerated remodeling of reformed motor end plates with VEGF treatment may impart enhanced functionality, as the formation of mature, singly innervated motor end plates is required for proper signaling.

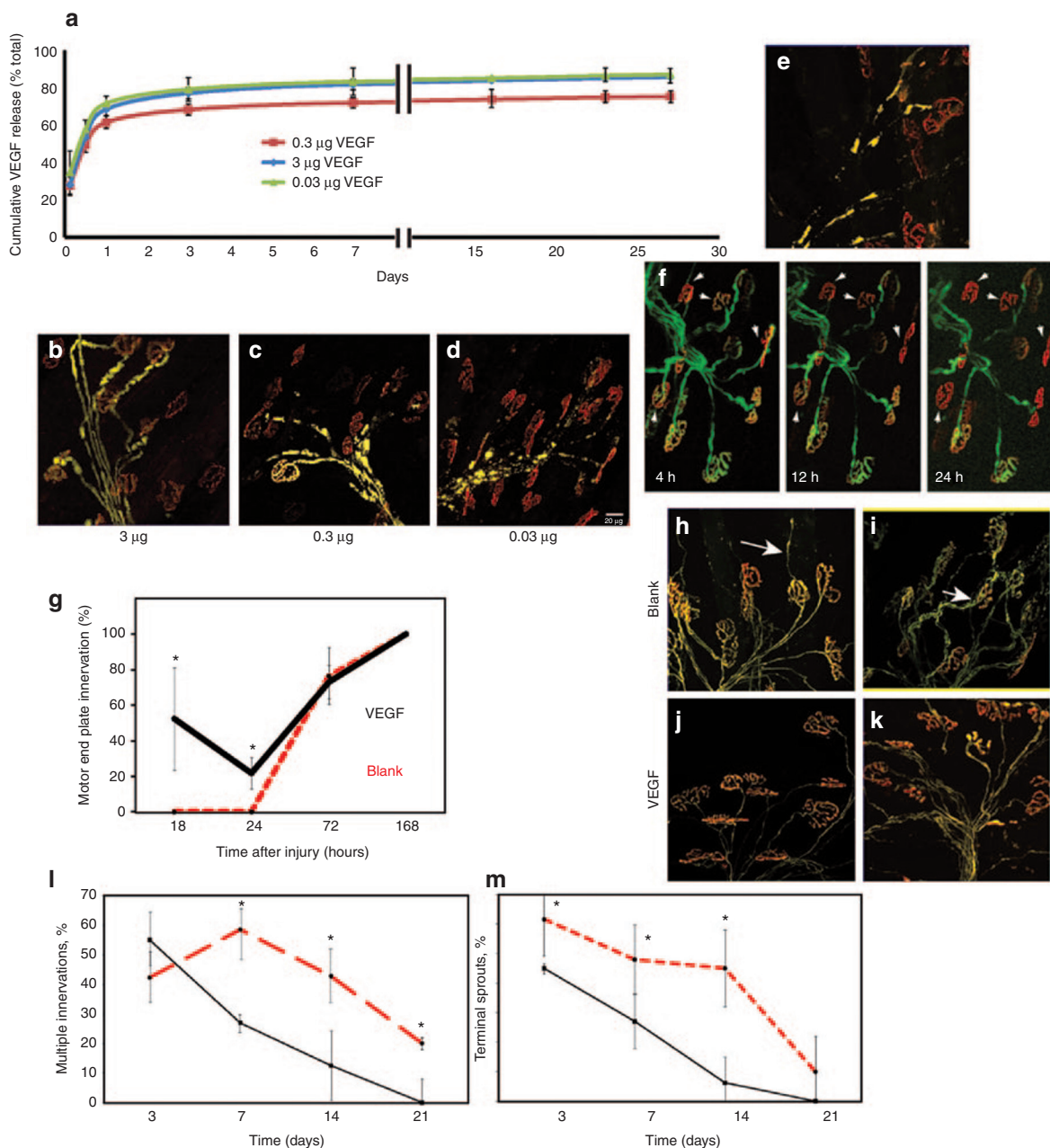


Figure 1 Gel-VEGF delivery slows axonal degeneration and promotes remodeling of newly formed neuronal end plates following double nerve crush with ischemia. **(a)** Release kinetics of vascular endothelial growth factor (VEGF) from gels. ^{125}I -labeled VEGF was used as a tracer to quantify release. **(b–d)** Sternomastoid muscle end-plate innervation at 24 hours following double crush with ischemia treated with alginate hydrogels containing 3, 0.3, or 0.03 micrograms of rhVEGF165 doses. Motor axons (yellow) and motor end plates (red) are shown. **(e)** Confocal micrographs of motor end plates 24 hours following double crush with ischemia, and no treatment, shows characteristic Wallerian neural degeneration of the yellow fluorescent protein (YFP)-labeled (yellow) motor axons, reducing the innervation of motor end plates (red). **(f)** Photomicrographs from specific time points during in situ time-lapse imaging of axons following double nerve crush with ischemia and delivery of VEGF-containing hydrogels. Individual arbors imaged at 4, 12, and 24 hours are shown, and arrowheads indicate motor end plates (red) that lose innervation (green) over the course of image collection. **(g)** Quantification of the percentage of total motor end-plate innervation following double crush with ischemia ($n = 3$, $*P < 0.05$). Confocal micrographs of neuromuscular junctions treated with either blank or VEGF-containing hydrogels at 7 **(h, i)** and 14 days **(j, k)** following injury demonstrate peripheral motor axons oversprouting and multiple innervation, with white arrows indicating **(h)** oversprouting axon and **(i)** multiple innervation. Quantification of **(l)** multiply innervated end plates and **(m)** terminal sprouts upon treatment with either blank (dotted line) or VEGF-containing (solid line) alginate hydrogels. Values represent the mean ($n > 50$ of motor end plates were analyzed), and error bars represent the standard deviations ($n = 3$, $*P < 0.05$).

VEGF delivery increases NGF and GDNF expression in ischemic muscle tissue

The impact of gel-VEGF delivery on innervation in a more extreme

ischemic injury model was next examined, where ischemic tibialis anterior (TA) muscle neural damage models neural and vascular injuries in injured human limbs.²¹ TA injury has a broad relevance

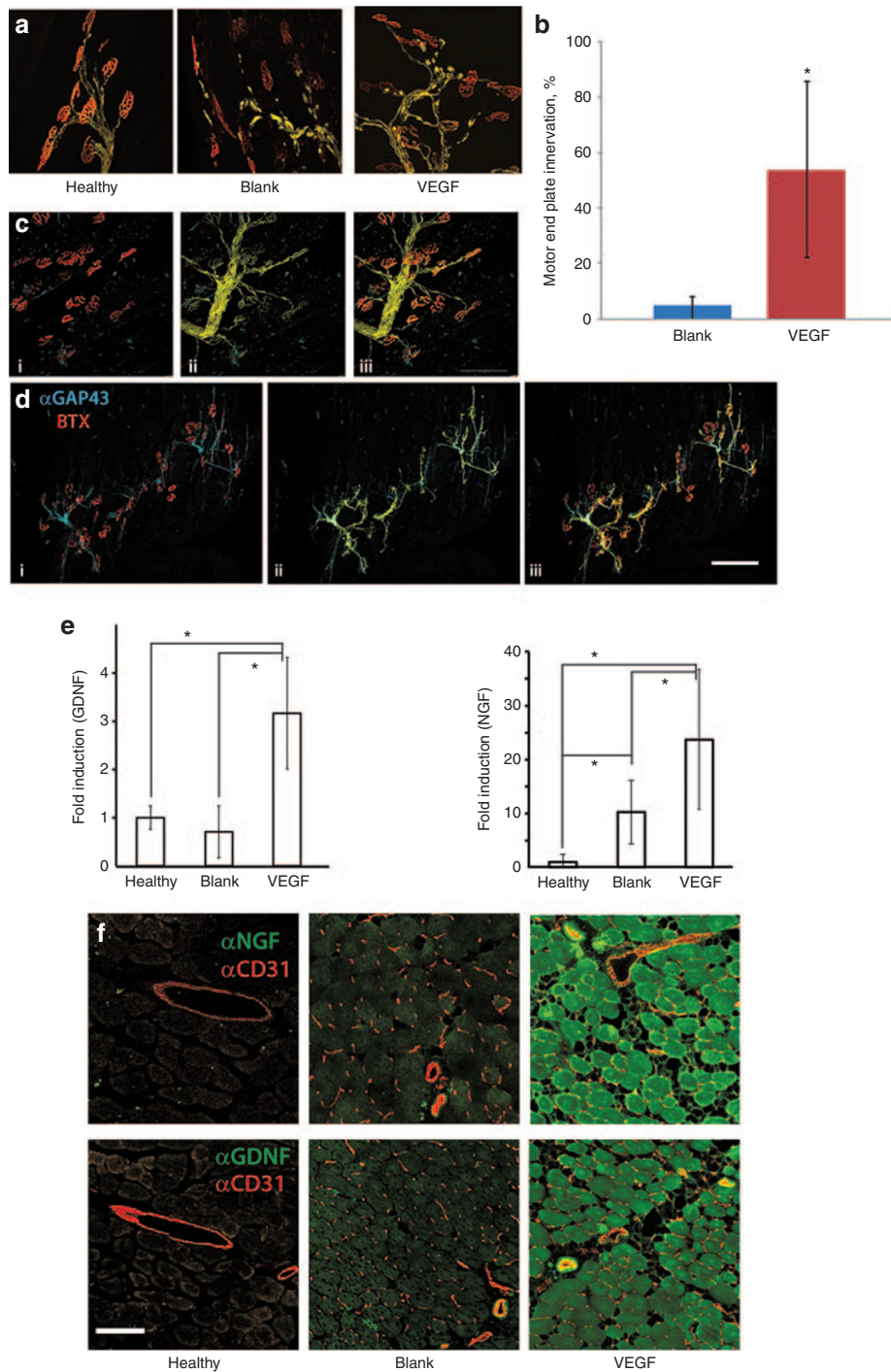


Figure 2 Exogenous vascular endothelial growth factor (VEGF) increases innervation in injured skeletal muscle and promotes expression of neurotrophic factors. **(a)** Representative images of healthy, blank gel (blank), or VEGF gel-treated (VEGF) tibialis anterior (TA) muscle in ischemic hindlimb of mice 7 days after injury. **(b)** Quantification of motor plate innervation in ischemic muscles on day 7 after injury ($n = 5$, $P < 0.05$). **(c)** Representative confocal images of healthy TA muscle and yellow fluorescent protein (YFP) axons **(ii)**, stained with motor end-plate marker (α -bungarotoxin, BTX, red, **i**) and GAP-43 antibody (blue, **i**, **ii**) and a combined image **(iii)**. Bar = 100 μ m. **(d)** Confocal tile scan of ischemic (day 7 after VEGF delivery) muscle region stained with bungarotoxin (red, **i**), GAP-43 antibody (blue, **i**, **ii**) with YFP axons (yellow, **ii**), and overlay **(iii)**. Bar 200 μ m. **(e)** Enzyme-linked immunosorbent assay for glial-derived neurotrophic factor (GDNF) and nerve growth factor (NGF) expression in healthy (control), blank gel-treated (blank), VEGF (VEGF) gel-treated TA lysates ($n = 4-5$, $*P < 0.05$). **(f)** Confocal scans of TA sections, stained with CD31 (PECAM-1, red), and anti-NGF or anti-GDNF IgG (green) on day 14 after injury. Representative images were taken from the ischemic muscle frozen sections of healthy or ischemic tissues, treated with blank hydrogels, hydrogels containing VEGF, and hydrogels with VEGF. Bar 200 μ m.

to muscle damage and neural degeneration occurring during peripheral arterial disorders. Ischemic injury in the TA hindlimb muscle was induced by femoral artery ligation. Previously, we have shown that VEGF delivery induces muscle regeneration in ischemic hindlimbs and results in restored blood supply at the affected skeletal muscles.¹⁴ TA innervation was analyzed similarly to the sternomastoid muscle model, although these muscles differ significantly in location, size, innervation, and fiber composition.¹⁴ Control ischemic muscles demonstrated wide-spread nerve degeneration, while partial innervation was observed in ischemic muscles supplemented with VEGF (**Figure 2a**). Quantification revealed that VEGF delivery resulted in 50% innervated motor end plates versus only 5% in the blank gel muscle samples on day 7 after the injury (**Figure 2b**). In order to differentiate motor axons maintained by the VEGF delivery from their regenerating counterparts, we stained for growth-associated protein (GAP-43), which serves as a distinctive marker of neural growth cones and extending axons.¹⁴ While motor axons in healthy TA muscles were not positively stained for GAP-43 (**Figure 2c**), as expected, two distinct populations were identified in VEGF-exposed ischemic muscles: one exhibiting positive staining for GAP-43 at axonal sprouts ($83 \pm 14\%$ of YFP-labeled axons) and another population negative for GAP-43 (**Figure 2d**). Both axon types exhibited similar morphology and innervation patterns (**Figure 2d**).

The levels in injured muscles of two of the key neurotrophic factors,²² NGF and glial-derived neurotrophic factor (GDNF), were next examined in TA tissue extracts, on day 14 after the ischemic insult and the hydrogel delivery, to determine if ischemia and/or injury impacted their expression. GDNF expression was not altered in injured muscle treated with blank gels, as compared to controls that were not injured (**Figure 2e**). In contrast, gel-VEGF delivery led to a significant increase of GDNF levels in the muscle tissue. NGF expression was significantly increased in ischemic muscles, as compared to uninjured muscle (**Figure 2e**), and, strikingly, gel-VEGF delivery led to a ~25-fold increase in NGF expression, as compared to noninjured muscle, and to a ~2.5-fold increase, compared to injured muscle (**Figure 2e**). Examination of frozen sections of TA muscles revealed that levels of both NGF and GDNF were slightly elevated upon the ischemic insult in blank gel-injected muscles, and appreciably elevated in VEGF-supplied muscles, with high expression in muscle fibers and some blood vessels (**Figure 2f**). The role of NGF and GDNF in VEGF-driven neural growth and maturation was next analyzed. Blocking exogenous VEGF activity with a neutralizing antibody, or

IgG-neutralization of NGF/GDNF expression, diminished innervation to blank gel levels (**Figure 3**). Specifically, when hVEGF IgG was applied with hVEGF-loaded gels, innervation levels were reduced to ~20% of healthy tissues, and when IgGs for either NGF or GDNF were delivered with VEGF-loaded gels, no innervation (0%) was observed.

To further examine the cell source of the observed increases in NGF/GDNF levels, primary mouse skeletal myoblasts were isolated from the mouse tissues, and primary human endothelial umbilical vein (HUVEC) or microvascular (HMVEC) cells were analyzed *in vitro* for NGF/GDNF expression and secretion. NGF and GDNF were detected in cultured myoblasts (**Supplementary Figure S1a,b**) and subjecting these cells to metabolic stress and hypoxia, combined with VEGF supplementation, led to a significant increase in NGF secretion (**Supplementary Figure S1c**). Both umbilical vein and microvascular endothelial cells also stained positive for NGF and GDNF (**Supplementary Figure S2**), secreting traceable amounts of NGF (10–20 pg/ml for HUVEC or HMVEC) both in normal conditions and with metabolic stress with VEGF supplementation growth conditions, although at much lower levels than myoblasts. Although GDNF expression was confirmed by immunohistochemistry in all of the cell cultures, no detectable GDNF secretion was observed in either myoblast- or endothelial cell-conditioned media. It must be noted, as no blocking IgGs were used to prevent a possible consumption of the expressed GDNF, that minimal levels of GDNF may have been secreted by the cells during the assay. The increased NGF expression with VEGF delivery may have therapeutic implications for the regeneration of sensory networks in transplanted tissues,²³ due to the susceptibility of sensory peripheral neurons to NGF signaling.²⁴ In addition, the prolonged increase in GDNF expression upon the VEGF delivery may also correlate with improved innervation and skeletal muscle fiber regeneration.²⁵

Restoration of blood supply in ischemic muscles, upon gel-VEGF delivery, is modulated via NGF/GDNF

Examination of vascular perfusion in untreated and gel-VEGF-treated ischemic muscles revealed an increase in perfusion over time with VEGF treatment (**Figure 4a**, graph), as expected.¹³ Surprisingly, blocking GDNF or NGF dissipated the positive effects of the VEGF delivery in restoring limb reperfusion (**Figure 4a**, graph), to a similar level as VEGF activity neutralization with a blocking antibody against the exogenous VEGF ligand (hVEGF). It has to be noted that the severity of limb necrosis in

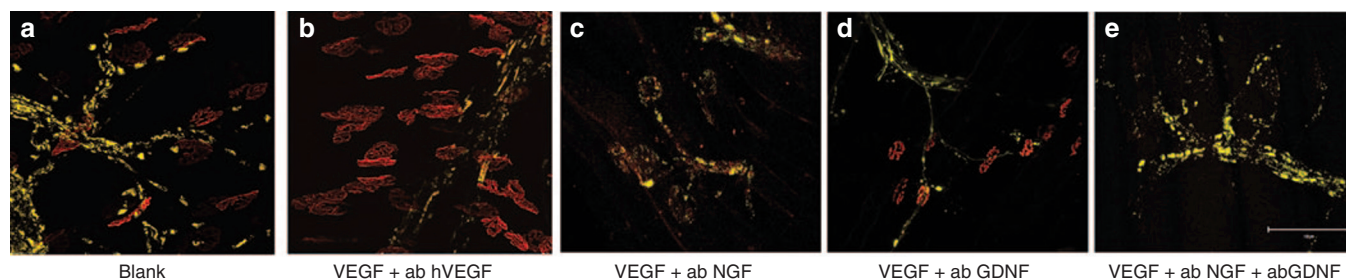


Figure 3 Vascular endothelial growth factor (VEGF) delivery maintains skeletal muscle innervation morphology via NGF/GDNF. (**a–e**) Representative images of ischemic muscle sections treated with combined delivery of VEGF and exogenous hVEGF165-neutralizing antibody (VEGF+ab hVEGF), or with VEGF and anti-NGF or anti-GDNF IgG. All images on day 7 after the ischemic injury. Bar 100 μ m.

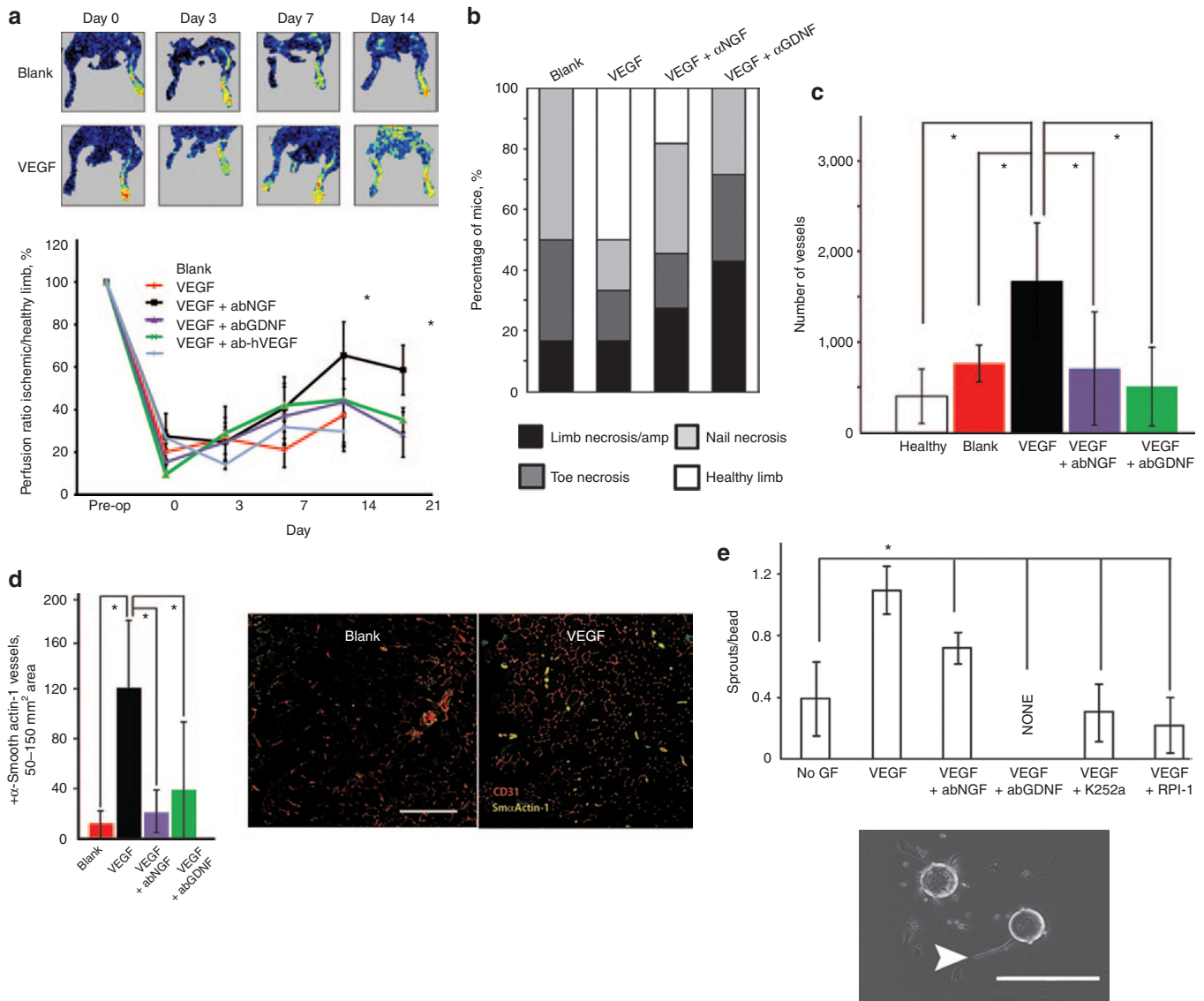


Figure 4 Gel-VEGF activates angiogenic processes in ischemic muscle, but blocking nerve growth factor (NGF) or glial-derived neurotrophic factor (GDNF) signaling diminishes vascular endothelial growth factor (VEGF) effects. **(a)** Representative color-coded images of blood perfusion in mouse hindlimbs, obtained using laser Doppler perfusion imaging. Left limb was ischemic, right normal, for both blank gel (blank) and VEGF-gel (VEGF)-treated mice. Imaging immediately after surgery (day 0) as compared to injured hindlimbs of the mouse at 3, 7, and 14 days after injury and treatment. Quantification of limb perfusion (graph) over time with treatments using blank (red), VEGF (black), VEGF with NGF-blocking IgG (purple), VEGF with GDNF-blocking IgG (green), and VEGF with hVEGF-neutralizing IgG (light blue) gels, ($n = 4-20$, $*P < 0.05$). **(b)** Scoring of the limb health on day 7 after the injury. **(c)** Total number of CD31-positive blood vessels (day 14 after the injury, $n = 4-8$, $*P < 0.05$). Data for healthy (white) and ischemic mice treated with gels as in **(a)**. **(d)** Total number of smooth muscle actin α -1 (SmaActin-1)-positive vessels for the same samples as in **(c)** ($n = 4-8$, $*P < 0.05$). Data for blank (red), VEGF-loaded (black) gel, or gels with either VEGF plus NGF IgG (purple) or VEGF plus GDNF (green) is shown. Representative images of CD31 (red) and SmaActin-1 (yellow) stained TA crosssections, on day 14 after the ischemic injury. Bar 200 μ m. **(e)** Sprouting ratios (upper panel) of endothelial cells grown in NO GF-media or media supplemented with VEGF, VEGF and NGF IgG, VEGF and GDNF IgG, VEGF and TrkA inhibitor (K252a), and VEGF and RET inhibitor (RPI-1). Inset shows representative phase-contrast image of endothelial cell sprout (white arrowhead). Sprouts are formed by cells migrating from microcarrier beads into fibrin gel. Bar = 400 μ m ($n = 4$, $*P < 0.05$, Students *t*-test).

these experiments required that a large proportion of the animals treated with blank gel and with VEGF-neutralizing IgGs be euthanized not later than day 14; therefore, no data are presented for these experimental conditions after this time point. Ischemic scoring of the injured limbs (**Figure 4b**, day 7) confirmed the positive role of sustained VEGF delivery in limb survival and confirmed the importance of NGF and GDNF in limb recovery with VEGF delivery. The severity of limb necrosis was greatly

reduced upon VEGF presentation, while blocking NGF/GDNF resulted in increased limb necrosis and amputations. Control experiments with VEGF hydrogels, supplemented with either goat or mouse anti-rabbit IgGs, led to similar rates of perfusion recovery as in limbs treated with VEGF gels only ($\sim 70\%$ perfusion recovery on 14 days from the ischemic injury, **Supplementary Figure S3**), confirming the specificity of findings with GDNF- and NGF-blocking antibodies. VEGF-supplemented TA samples

demonstrated a significant increase in the number of blood vessels (Figure 4c), as compared to healthy muscles. Blocking NGF or GDNF activity reduced capillary numbers to control levels, even with VEGF delivery (Figure 4c). Histological analysis of blood vessel size distribution in injured TA muscle samples after 14 days (Supplementary Figure S3), showed a noticeable shift in the size of the CD31-positive blood vessels, and the average vessel area was significantly increased by exogenous VEGF at this time, while blocking NGF/GDNF reduced the average area of the vessels to the blank-gel condition (Supplementary Figure S3).

The impact of NGF and GDNF in blood vessel maturation was next assessed. We have shown previously that sustained VEGF delivery results in increased blood vessel maturation, as marked by smooth muscle actin staining of blood vessels.²⁶ When the number of mature blood vessels in ischemic TA cross-sections, as indicated by positive staining for smooth muscle actin-1 expression (Figure 4d inserts), was quantified, VEGF delivery led to a significant increase by 2 weeks as expected (Figure 4d). Importantly, blocking NGF or GDNF when VEGF was delivered from hydrogels, reduced the number of mature blood vessels to the level observed for the blank-gel treated ischemic TA muscle (Figure 4d).

To better characterize the role of VEGF receptors and impact of NGF/GDNF signaling on VEGF-driven angiogenesis, a 3D *in vitro* model of sprouting angiogenesis²⁷ was used to quantify endothelial cell sprouting with NGF or GDNF blockade (Figure 4e). Blocking either NGF or GDNF ligands with antibodies, or interfering with their signaling pathways (trkA²⁸- and RET²⁹-mediated signaling respectively), significantly reduced endothelial cell sprouting. Strikingly, no sprouts were formed when GDNF-blocking IgG was present. Endothelial cell viability was maintained in the presence of either NGF- or GDNF-blocking antibodies (Supplementary Figure S4a). In subsequent control experiments, neither NGF nor GDNF supplementation induced sprout formation (Supplementary Figure S4b). Blocking NGF activity alone had no significant effect on sprout formation when compared to basal growth media. When GDNF IgGs were present in fibrin gels and growth media, HUVECs remained rounded and attached to the microspheres (Supplementary Figure S4b insert) and no sprouts formed regardless of the VEGF supplementation. When VEGF was delivered with either control mouse or rabbit IgGs, as in Supplementary Figure S3 sprouting ratios were similar to VEGF-induced levels.

DISCUSSION

Altogether, the findings of this study indicate that gel-VEGF delivery following ischemic muscle injury dramatically slows neuron degeneration and promotes regeneration. Our observations suggest that the effects of VEGF delivery are modulated, at least in part, via induced expression of GDNF and NGF in skeletal muscle fibers and endothelial cells. The linkage between VEGF supplementation and elevated levels of NGF and GDNF in skeletal muscles is reported here, indicating critical roles of NGF and GDNF in tissue reperfusion following injury, and demonstrate a strong dependence of endothelial cell sprouting, induced by VEGF, on NGF and GDNF signaling. Together, these data provide a possible link between vascular and neural networks during the course

of tissue regeneration. As an approach to manipulate the VEGF-NGF-GDNF signaling nexus, alginate hydrogels are attractive materials for exogenous VEGF delivery.

The effects of gel-VEGF delivery on axon regeneration were examined at the NMJ, for the evaluation of terminal axon regeneration, and these studies revealed that exogenous VEGF delayed axonal degeneration following neuronal crush and ischemic injury and promoted more rapid regeneration. Under ischemic conditions, VEGF released from endothelial or glial cells has been shown to directly stimulate proliferation of neural progenitor cells and to provide neuroprotection of adult neurons; VEGF can also stimulate neural progenitor cells survival.⁷ In sciatic nerve defects, VEGF promoted axon outgrowth across the defect. Treating amyotrophic lateral sclerosis-like diseased mice with VEGF has been shown to have a direct neuroprotective effect on motor neurons,³⁰ and the growth cones of regenerating axons have been shown to express VEGF receptors.⁵ While distal maintenance of ischemic axons does not imply enhanced functionality since those axons cannot reconnect to the cell body to resume signaling, VEGF delivery may also modulate synapses dependent on VEGF signaling.³¹ This ability of VEGF to maintain synapses that would otherwise be lost due to changes at the motor end plates, which also may occur in neurodegeneration and as a result of aging,⁶ may have therapeutic implications.

Our findings establish a correlation between the sustained presentation of recombinant VEGF to injured or ischemic tissues and cells and the expression of neurotrophic factors. VEGF is a potent activator, controlling endothelial cell survival, migration, and formation of angiogenic sprouts, and is tightly controlled by the local oxygen levels both during the developmental and adult stages of tissue growth and organ formation.³² Migrating endothelial cells can provide temporal survival cues for developing neurons and are capable of sustaining their growth, before the establishment of a functional blood supply.³³ The role of VEGF in supporting the functional crosstalk between the vascular and neural networks, sustaining the integrity of neuroeffector junctions between the axons and blood vessels smooth muscle cells, suggested that additional factors may have a role in these interactions.³⁴ Previous studies also reported a crosstalk between VEGF and GDNF during the early kidney development, indicating the importance of interactions between neural and vascular signaling pathways.³⁵ The significant increase in levels of NGF and GDNF in VEGF-treated muscles and VEGF-exposed myogenic and endothelial cells in culture supports a mechanism of VEGF-induced expression of neurotrophic factors. Our findings suggest that the major source for the observed increase in NGF levels with VEGF delivery to ischemic skeletal muscles are the muscle cells, as myoblasts show ~10-fold higher levels of *in vitro* NGF secretion when compared to other cell types.

A remarkable finding in these studies was blocking GDNF completely abrogated angiogenesis *in vitro* and *in vivo* while blocking NGF partially inhibited angiogenesis. Endothelial cells have been shown to express NGF and its receptors and demonstrated NGF-dependent migration.⁵ GDNF/GDNF receptor expression was previously reported in muscle fibers³⁶ and capillary endothelial cells,³⁷ where it plays a critical role in the formation of the blood-brain barrier. NGF is expressed by skeletal muscles

and is elevated following injection of the inflammatory cytokine TNF- α .³⁸ The NGF receptor *trkA* is also expressed by skeletal muscle tissues.³⁶ While previous reports indicated a critical role for NGF in early angiogenesis and later blood vessel maturation,⁵ we show that NGF alone is not sufficient for the induction of endothelial sprouting, it instead requires initiation by VEGF signaling. A close correlation between VEGF and NGF signaling during vessel growth, branching, and endothelial sprouting has been previously reported.⁵ Our findings suggest that both in sprouting *in vitro* and during ischemic recovery, both factors interact at the endothelial cell level. Importantly, we now report that GDNF plays a similarly critical role in the formation of vascular networks in skeletal muscles that are induced by the VEGF signaling. The direct effect of GDNF on reperfusion may be attributed to the lack of endothelial cell sprouting when GDNF activity is blocked. The role of GDNF in endothelial cell adhesion and migration, leading to the restoration of functional vasculature may be translated via integrin β 1 adhesion proteins, since it was reported to be one of the signaling partners for GDNFR α -1³⁹ and is also a critical protein in vascular patterning and postnatal remodeling.⁴⁰ Our results also correlate with recent findings of a GDNF role in skin *de novo* blood vessel formation, also supporting signaling interactions between the neural and vascular systems.⁴¹ Thus, NGF and GDNF, having similar effects on perfusion recovery of the ischemic limbs, may act via different signaling cascades in endothelial cells.

Critical challenges still exist in regeneration of sensory networks in transplanted tissues²³ and gel-VEGF delivery may have utility, harnessing the susceptibility of sensory peripheral neurons to NGF signaling.⁴² While NGF activity was shown to be critical for axonal spouting,⁴³ studies with overexpressed GDNF in skeletal muscles have shown a significant elevation of cholinesterase-positive end plates in muscle fibers.⁴⁴ A recent study has also indicated strong synergistic effects of VEGF and GDNF in the prolonged survival of muscle motor end plates and motor neurons in a rat amyotrophic lateral sclerosis model of disease.⁴⁵ These findings suggest that the observed increase in the expression of both factors upon VEGF delivery plays a critical role in the maintenance and the *de novo* formation of motor axon units in ischemic skeletal muscles.

Alginate hydrogels are attractive materials for exogenous VEGF delivery, as they provide a localized release at therapeutic doses for several weeks, and are capable of confining the critical VEGF concentrations to the site of injury for significant periods of time,¹³ as opposed to the minimal effects of bolus VEGF delivery.^{13,14,16} Tissue regeneration following injury occurs over a period of days to weeks, which likely leads to a requirement for the prolonged presence of signaling molecules. These gels also allow minimally invasive injections to a specific site.¹³ The role of sustained release has not been previously appreciated in investigations using VEGF as a therapeutic target in peripheral nervous system repair.⁵ Further, VEGF delivery has been previously demonstrated to lead to multiple regenerative outcomes, ranging from endothelial cell recruitment to activation of processes, such as *de novo* bone formation⁴⁶ and muscle fiber regeneration.¹⁴ The VEGF-dependent effects on muscle regeneration resulted in myogenic cell activation and proliferation, where Pax7 and myogenin-positive cell levels were elevated and a significant proportion of regenerating muscle fibers demonstrated centrally localized nuclei.¹⁴ The specific timepoint for the analysis of

innervation in the present study (day 7 postinjury) was chosen as it has been reported that the initial gene activation, which leads to muscle repair, is concluded after 7 days.⁴⁷ It is likely to be critically important to maintain the presence of VEGF throughout the early stages of regeneration, where an array of developmental factors (e.g., IGF-1)⁴⁷ can provide a synergistic effect with the exogenous VEGF. The later time point of study (day 14) was chosen due to the reported increase in VEGF-induced perfusion, and muscle fiber regeneration and reinnervation¹⁴ of ischemic skeletal muscles at this time.

A striking finding of the present studies is that NGF and GDNF play important roles in VEGF-driven revascularization of ischemic muscle, including endothelial cell sprouting and blood vessel maturation. Inhibition of NGF and GDNF in the presence of VEGF stimulation diminished the formation of capillaries and their adaptation into larger vessels, reduced recovery of limb perfusion, and led to increased limb necrosis. These results, summarized in a model of VEGF-induced angiogenesis and neural regeneration in skeletal muscles (**Supplementary Figure S5**), suggest that NGF and GDNF have roles in blood vessel growth and maturation in skeletal muscles. Therefore, we propose that VEGF supplementation results in angiogenic and neurogenic responses, either directly affecting axonal growth, or indirectly via increased expression of angioneurins,⁵ such as NGF and GDNF, by the proliferating vasculature. The potency of these responses may vary between tissues, stages of regeneration and prevalence of either component at the specific site of repair.

MATERIALS AND METHODS

Formulation of polymeric scaffolds. Ultrapure alginates were purchased from ProNova Biomedical AS (Oslo, Norway). MVG alginate, a high-G-containing alginate (M/G ratio of 40/60 as specified by the manufacturer) was used as the high molecular weight (molecular mass 250 kDa) component to prepare gels, as described previously.¹³ LMW alginate (molecular mass 50 kDa) was obtained by irradiating high molecular weight alginate with a cobalt-60 source for 4 hours at a dose of 5.0 Mrad.

The alginate used to form gels was a combination of the two different molecular weight polymers at a ratio of 3:1. Both alginate polymers were diluted to 1% w/v in double-distilled H₂O, and 1% of the sugar residues in the polymer chains were oxidized with sodium periodate (Sigma-Aldrich, St Louis, MO) by maintaining solutions in the dark for 17 hours at room temperature, as previously described.²⁰ An equimolar amount of ethylene glycol (Fisher, Pittsburgh, PA) was added to stop the reaction, and the solution was subsequently dialyzed (MWCO 1000, Spectra/Pore) over 3 days. The solution was sterile filtered, frozen (−20 °C overnight), lyophilized, and stored at −20 °C. To prepare blank gels, modified alginates were reconstituted in EGM-2 basal media (Lonza, Frederick, MD) to obtain 2% w/v alginate solutions prior to gelation. The alginate solutions were crosslinked with aqueous slurries of a calcium sulfate solution (0.21 g CaSO₄/1 ml distilled H₂O) at a ratio of 25:1 (40 μ l of CaSO₄ slurry per 1 ml of 2% w/v alginate solution) using a 1-ml syringe. Reconstituted alginate was stored at 4 °C.

VEGF-containing hydrogels were formed by mixing 2.3% low MW alginate solution with 1 mg/ml rhVEGF₁₆₅ (National Cancer Institute, Bethesda, MD) in phosphate-buffered saline (PBS) solution to form a 2% solution prior to the addition of high MW alginate and calcium crosslinking agent. Hydrogels were allowed to cure at 4 °C for at least 30 minutes before use.

Growth factor incorporation and release kinetics. ¹²⁵I-labeled VEGF₁₆₅ was purchased from PerkinElmer Life Sciences (Wellesley, MA). Alginates were mixed with the ¹²⁵I-VEGF₁₆₅ as described above to quantify VEGF release *in vitro*. The resulting mixture was cast between two glass plates

separated with 1-mm spacers and allowed to gel for 30 minutes. The gels were divided into four samples and subsequently incubated in 3 ml of PBS, pH 7.2 (Invitrogen, Carlsbad, CA) with 0.1 g/l of $MgCl_2 \cdot 6H_2O$ and 0.132 g/l of $CaCl_2 \cdot 2H_2O$ (Sigma-Aldrich) in a 37 °C humidified incubator. At each experimental time point, the radiolabeled growth factor present in the buffer solution was measured using a gamma counter (1470 WIZARD; PerkinElmer). VEGF cumulative release was calculated as in a previous study,¹³ comparing with the initial total ^{125}I -VEGF₁₆₅ incorporated into the gel sample.

Sternomastoid muscle ischemic injury. All animal studies and husbandry were performed according to the protocols and guidelines of the Institutional Animal Care and Use Committee at Harvard University. C57Bl/6J mice and transgenic YFP16 mice (genetic background of C57Bl/6 strain, selectively expressing YFP under control of a *thy-1* promoter in motoneurons)¹⁵ were anesthetized with an intraperitoneal injection of a ketamine (17.39 mg/ml) and xylazine (2.61 mg/ml) cocktail; neck hair was removed with a depilatory, and a midline incision was made from the mandible to the sternum. The sternomastoid muscle was exposed by reflection of the salivary glands and surrounding connective tissue, and the nerve was exposed at its point of emergence from under the digastric muscle and lesioned by crushing with forceps until the nerve appeared clear. The incision was sutured, and the animal was allowed to recover for 3 days, at which time, a repeat incision was made in the neck, and the crush was repeated. For ischemic injury of sternomastoid muscle, the sternocleidomastoid vessel was ligated with a nondegradable nylon suture (5-0 Ethilon; Ethicon, Somerville, NJ) at the time of the second crush.

Tibialis anterior muscle ischemic injury. Hindlimb ischemia was induced by unilateral external iliac and femoral artery and vein ligation, as previously described.¹⁴ Briefly, animals were anesthetized by intraperitoneal injection of a ketamine (17.39 mg/ml) and xylazine (2.61 mg/ml) cocktail. The entire hindlimb was shaved and sterilized prior to making an incision through the dermis. The external iliac artery and vein, and the femoral artery and vein were ligated using nondegradable nylon suture. The vessels were severed between the ligation points, and blank or VEGF-containing hydrogel (3 µg VEGF/50 µl gel) was injected at the muscle tissue adjacent to the TA muscle.

Hydrogel delivery. Either blank, hVEGF₁₆₅-containing (3 µg VEGF/gel) or human VEGF-neutralizing (AF-293-NA, delivered in 1:1 stoichiometric ratio with hVEGF ligand) were from R&D Systems (Minneapolis, MN); GDNF- (ab89341, Abcam, Cambridge, MA) or NGF-neutralizing IgGs (ab6199, Abcam)-containing hydrogels were implanted by injecting 50 µl of the crosslinked hydrogel into the connective tissue space adjacent to the TA muscle. The incision was closed and the animal was allowed to recover.

In vivo imaging of innervations at muscle end plates. Adult mice were anesthetized as above and intubated with a plastic tube connected to a small animal ventilator (SAR-830/P, SWE Inc, Ardmore, PA). The sternomastoid muscle was exposed and stabilized on polished metal platform as previously described. Postsynaptic sites were labeled by adding a nonsaturating dose (0.1 µg/ml for 30 minutes) of Alexa647-conjugated α -bungarotoxin (Invitrogen) to the end-plate band. Pre- and postsynaptic structures were simultaneously imaged using a water immersion objective ($\times 20$, 0.5NA) in a confocal microscope (Zeiss 510 Meta; Carl Zeiss, Thornwood, NY). After imaging, the neck was closed with sutures and the animal was returned to the cage for recovery. Several hours later, the animal was reanesthetized and the same junctions were reimaged. Maximum intensity projections were rendered using Zen software (Zeiss).

Laser doppler perfusion imaging. Animals ($n = 4-20$ per experimental condition) were anesthetized with isoflurane (2%v/vO₂), and hindlimb blood flow was measured for the ischemic and healthy limbs with the Periscan blood perfusion laser scanning monitor (Perimed, Järfälla, Sweden). Time

points for each measurement were selected immediately after the ischemic injury, day 3, 7, 14 and day 21 postinjury. Perfusion ratios were obtained by dividing the blood perfusion intensity in the whole region of interest in the ischemic limb to the same area in the contralateral, unoperated limb.

Tissue extraction. At time points of 18 hours, 1 and 3 days, and 1, 2, and 3 weeks, as measured from the time of the surgery, mice were anesthetized by an intraperitoneal injection of sodium pentobarbital (60 mg/ml) and fixed by transcardial injection of 4% paraformaldehyde. The sternomastoid and TA muscles (depending on the model) were explanted, dissected to remove any connective tissue, and postfixed in 4% paraformaldehyde for 30 minutes.

Immunohistochemistry for tissue cryosections, floating tissue sections, and fixed cells. Fixed muscles were incubated first in PBS with 5% sucrose solution for 2 hours in room temperature; samples were incubated overnight in 20% sucrose/PBS hypertonic solution. After embedding in optimal cutting temperature cryoprotection compound and snap freezing in liquid nitrogen, sample molds were kept at -80 °C. Prior to sectioning, samples were equilibrated in the cryostat (Leica Microsystems, Buffalo Grove, IL) chamber at -22 °C. Ten micrometer sections were mounted on glass slides and kept at -20 °C prior to immunostaining. For the immunostaining of the frozen sections, samples were equilibrated to ambient temperature, air dried and washed with PBS. Antigen blocking of the samples was done with PBS containing 1% (w/v) of bovine serum albumin (BSA) Fraction V (Roche Applied Sciences, Indianapolis, IN) with the addition of normal goat serum (10%, v/v) for 1 hour at room temperature. Primary antibodies were diluted in PBST/BSA buffer (PBS with 0.01 %Tween-20 v/v, with 1%BSA w/v) and allowed to bind overnight at 4 °C in a humidified chamber. After washing three times with PBS, secondary antibodies were diluted in PBS/BSA buffer and applied for 1 hour at room temperature. After three washes with PBS, samples were air dried and mounted (ProLong Gold Antifade; Invitrogen). Anti-SmActin-1 rabbit IgG (1:100 dilution; Abcam) and anti-CD31 (Rat IgG, 1:250 dilution; BD Biosciences, San Jose, CA) were used.

For the analysis of neuromuscular innervation, 100-µm-thick longitudinal sections were cut with a vibrating microtome (Leica) from the fixed and sucrose-equilibrated muscle samples and kept in PBS at 4 °C prior to staining. After rinsing with PBS, muscles were stained with Alexa 594-bungarotoxin (Invitrogen) to visualize acetylcholine receptors at muscle motor end plates. Samples were produced both from C57Bl/6J mice and YFP 16 mice, which do not require immunostaining of the neural sprouts. Sections from C57Bl/6J were floated in the appropriate buffers, with antigen retrieval and blocking done with 0.3% Triton X-100 (v/v) and 10% normal goat serum (v/v). GAP-43 stain was done with rabbit anti-GAP-43 IgG (AB5220 1:500 dilution, Millipore, Billerica, MA) and visualized by the secondary labeling with Alexa647 goat anti-rabbit IgG (4 µg/ml, Invitrogen). After completion, samples were mounted on glass slides, air dried, and sealed with mounting media. Confocal z-stacks were obtained using a LSM 710 microscope (Zeiss), and maximum intensity projections images were analyzed. Reinnervation was quantified by counting the sites of overlap of motor neuron axons (yellow) and end plates (red). The morphologies of terminal sprouts and oversprouting levels, where axons continued their growth beyond the motor end plates, and multiple innervations, characterized by several axonal branches converging at the individual end plate, were assayed by counting all NMJs receptor sites in which more than one axon converged. At least 50 motor end plates were counted for each condition.

Blood vessel analysis in TA muscle sections. Frozen TA sections (10 µm thickness) were stained with primary antibodies, anti-CD31 (Rat IgG; BD Biosciences, 1:100 dilution), anti SmActin (Rabbit IgG; Abcam, 1:100), and after labeling with Alexa647 Goat anti-Rat and Alexa 546 goat anti-rabbit IgGs (Life Technologies, 1:400 dilution), tile scans of the whole sample area were obtained with LSM 710 confocal microscope. Color tile scan images were processed in ImageJ software (National Institutes of Health, Bethesda, MD), by background reduction and threshold levels function, and CD-31

and smooth muscle actin-1 (SmActin) positive objects were counted using ImageJ software, where any object with object area larger than 5 μm^2 was counted as a capillary. The total numbers of CD31 or SmActin objects were obtained after normalization to the each sample area, and their distribution was calculated within the 5–250 μm object area size.

In vitro sprouting assay. The sprouting assay was adapted from previously described methods.¹⁶ Briefly, swollen and sterilized dextran microcarriers (Amersham Biosciences, Piscataway, NJ) were washed in EGM-2 and combined with human umbilical vein endothelial cells (passage 4–6, Lonza, Frederick, MD) in a spinner flask. The flask was alternated between stirring and nonstirring every 30 minutes and incubated at 37 °C and 5% CO₂ to promote even cell attachment. After 4 hours, the beads and cells were left stirring for additional 20 hours. The cell-coated beads were then collected and incubated in flasks on a shaker for 1–2 days until cells became confluent on the beads. A fibrinogen-bead solution (1 ml of cell-coated beads in media, 27% w/v fibrinogen, and 0.5% w/v aprotinin) was then mixed with a thrombin solution (8.3 U/ml thrombin) in each well 12-well tissue culture plate at a ratio of 5:4 fibrinogen-bead solution: thrombin solution. Gels were allowed to set in the incubator for 20 minutes before addition of basic EGM-2 supplemented with factors of interest at specific concentrations. NGF IgG (2 μg /well rabbit or mouse IgG, Abcam), GDNF IgG (2 μg /well rabbit IgGs, Abcam, Genetex (Irvine, CA) or Biovision (Milipitas, CA)), human VEGFR-1 or human VEGFR-2-neutralizing IgGs (2 μg /well, AF321 or AF357, R&D Systems), and Rabbit anti-Human or Mouse anti-Rabbit Iggs (2 μg /well, Jackson ImmunoResearch, West Grove, PA) were mixed with thrombin solution in wells. VEGF (50 ng/ml), NGF (20 ng/ml), or GDNF (20 ng/ml) were added to the EGM-2 media without growth factors, media were changed every 24 hours, and gels were maintained for up to 72 hours. Inhibitors of trkA receptor (NGF pathway, K252a, 100 (nmol/l)/ml, Sigma-Aldrich) or RET receptor (GDNF pathway, RPI-1, 20 (mmol/l)/ml, Sigma-Aldrich) were added to growth media. Gels were rinsed with PBS and fixed with 4% paraformaldehyde before imaging for sprout quantification. A sprout was defined as at least two continuous cells extending into the surrounding gel from the microcarrier bead. Sprouting ratios were determined by dividing the manual counts of sprouts by bead count (>100 in each well, $n = 6$ in each condition).

Statistical analysis. *In vitro* data were analyzed by Student's *t*-test (two-tailed standard distribution, $P < 0.05$, considered to be statistically significant). *In vivo* experiments ($n = 4$ –20 animal samples for each experimental condition) were compared using Student's *t*-test (enzyme-linked immunosorbent assay, laser doppler perfusion imaging, SmActin-positive vessels), analysis of variance analysis (motor end plate innervation), and Wilcoxon signed-rank test (blood vessel amount and area size). Asterisks indicate $P < 0.05$.

SUPPLEMENTARY MATERIAL

Figure S1. VEGF delivery and metabolic stress induce NGF and GDNF expression in cultured primary skeletal myoblasts.

Figure S2. Endothelial cells express NGF and GDNF under metabolic stress conditions with VEGF supplementation.

Figure S3. VEGF delivery increases blood vessel size in ischemic skeletal muscles, and non-specific IgG controls do not interfere with VEGF-induced perfusion recovery.

Figure S4. VEGF activates endothelial sprout formation prolonged via VEGFR-1 via with NGF and GDNF regulation.

Figure S5. Model of VEGF impact on neural and vascular regeneration in injured skeletal muscles.

ACKNOWLEDGMENTS

We thank the Biological Resources Branch of the National Cancer Institute for providing VEGF for the studies, and Emily Savage for her help with *in vitro* studies. This study was supported by National Institutes

of Health Grants R01 DE013349 and R43AG029705, and European Molecular Biology Organization (EMBO) Long-Term Fellowship ALTF 42–2008. D.S., H.S., H.H.V., J.W.L., and D.J.M. designed research; D.S., H.S., K.L., C.M., J.C.T., C.K., Y.B., N.H., C.C., and J.K. performed research; E.A. contributed modeling tools; D.S. and H.S. analyzed data; and D.S. and D.J.M. wrote the paper.

REFERENCES

- Nguyen, QT, Sanes, JR and Lichtman, JW (2002). Pre-existing pathways promote precise projection patterns. *Nat Neurosci* **5**: 861–867.
- Said, G (2007). Diabetic neuropathy—a review. *Nat Clin Pract Neurol* **3**: 331–340.
- Tuszynski, MH and Steward, O (2012). Concepts and methods for the study of axonal regeneration in the CNS. *Neuron* **74**: 777–791.
- Snider, WD, Zhou, FQ, Zhong, J and Markus, A (2002). Signaling the pathway to regeneration. *Neuron* **35**: 13–16.
- Carmeliet, P and Tessier-Lavigne, M (2005). Common mechanisms of nerve and blood vessel wiring. *Nature* **436**: 193–200.
- Ferrara, N (2002). Role of vascular endothelial growth factor in physiologic and pathologic angiogenesis: therapeutic implications. *Semin Oncol* **29**(6 suppl. 16): 10–14.
- Schraatzberger, P, Schraatzberger, G, Silver, M, Curry, C, Kearney, M, Magner, M *et al.* (2000). Favorable effect of VEGF gene transfer on ischemic peripheral neuropathy. *Nat Med* **6**: 405–413.
- Storkebaum, E and Carmeliet, P (2004). VEGF: a critical player in neurodegeneration. *J Clin Invest* **113**: 14–18.
- Siemionow, MZ, Zor, F and Gordon, CR (2010). Face, upper extremity, and concomitant transplantation: potential concerns and challenges ahead. *Plast Reconstr Surg* **126**: 308–315.
- Eppler, SM, Combs, DL, Henry, TD, Lopez, JJ, Ellis, SG, Yi, JH *et al.* (2002). A target-mediated model to describe the pharmacokinetics and hemodynamic effects of recombinant human vascular endothelial growth factor in humans. *Clin Pharmacol Ther* **72**: 20–32.
- Epstein, SE, Kornowski, R, Fuchs, S and Dvorak, HF (2001). Angiogenesis therapy: amidst the hype, the neglected potential for serious side effects. *Circulation* **104**: 115–119.
- Silva, EA and Mooney, DJ (2010). Effects of VEGF temporal and spatial presentation on angiogenesis. *Biomaterials* **31**: 1235–1241.
- Silva, EA and Mooney, DJ (2007). Spatiotemporal control of vascular endothelial growth factor delivery from injectable hydrogels enhances angiogenesis. *J Thromb Haemost* **5**: 590–598.
- Borselli, C, Storie, H, Benesch-Lee, F, Shvartsman, D, Cezar, C, Lichtman, JW *et al.* (2010). Functional muscle regeneration with combined delivery of angiogenesis and myogenesis factors. *Proc Natl Acad Sci USA* **107**: 3287–3292.
- Feng, G, Mellor, RH, Bernstein, M, Keller-Peck, C, Nguyen, QT, Wallace, M *et al.* (2000). Imaging neuronal subsets in transgenic mice expressing multiple spectral variants of GFP. *Neuron* **28**: 41–51.
- Chen, RR, Silva, EA, Yuen, WW, Brock, AA, Fischbach, C, Lin, AS *et al.* (2007). Integrated approach to designing growth factor delivery systems. *FASEB J* **21**: 3896–3903.
- Lichtman, JW, Magrassi, L and Purves, D (1987). Visualization of neuromuscular junctions over periods of several months in living mice. *J Neurosci* **7**: 1215–1222.
- Gillingswater, T and Ribchester, R (2003). The relationship of neuromuscular synapse elimination to synaptic degeneration and pathology: Insights from the Wlds and ohter mutant mice. *J Neurocytol* **32**: 863–881.
- Carmeliet, P and Jain, RK (2011). Molecular mechanisms and clinical applications of angiogenesis. *Nature* **473**: 298–307.
- Sanes, JR and Lichtman, JW (1999). Development of the vertebrate neuromuscular junction. *Annu Rev Neurosci* **22**: 389–442.
- Couffignal, T, Silver, M, Zheng, LP, Kearney, M, Witzensbichler, B and Isner, JM (1998). Mouse model of angiogenesis. *Am J Pathol* **152**: 1667–1679.
- Zhao, C, Veltri, K, Li, S, Bain, JR and Fahnestock, M (2004). NGF, BDNF, NT-3, and GDNF mRNA expression in rat skeletal muscle following denervation and sensory protection. *J Neurotrauma* **21**: 1468–1478.
- Siemionow, M and Ozturk, C (2012). Face transplantation: outcomes, concerns, controversies, and future directions. *J Craniofac Surg* **23**: 254–259.
- Lee, KF, Li, E, Huber, LJ, Landis, SC, Sharpe, AH, Chao, MV *et al.* (1992). Targeted mutation of the gene encoding the low affinity NGF receptor p75 leads to deficits in the peripheral sensory nervous system. *Cell* **69**: 737–749.
- Suzuki, H, Hase, A, Kim, BY, Miyata, Y, Nonaka, I, Arahata, K *et al.* (1998). Up-regulation of glial cell line-derived neurotrophic factor (GDNF) expression in regenerating muscle fibers in neuromuscular diseases. *Neurosci Lett* **257**: 165–167.
- Richardson, TP, Peters, MC, Ennett, AB and Mooney, DJ (2001). Polymeric system for dual growth factor delivery. *Nat Biotechnol* **19**: 1029–1034.
- Nehls, V and Drenckhahn, D (1995). A novel, microcarrier-based *in vitro* assay for rapid and reliable quantification of three-dimensional cell migration and angiogenesis. *Microvasc Res* **50**: 311–322.
- Takahashi, M (2001). The GDNF/RET signaling pathway and human diseases. *Cytokine Growth Factor Rev* **12**: 361–373.
- Nakamura, K, Tan, F, Li, Z and Thiele, CJ (2011). NGF activation of TrkA induces vascular endothelial growth factor expression via induction of hypoxia-inducible factor-1 α . *Mol Cell Neurosci* **46**: 498–506.
- Storkebaum, E, Lambrechts, D, Dewerchin, M, Moreno-Murciano, MP, Appelmans, S, Oh, H *et al.* (2005). Treatment of motoneuron degeneration by intracerebroventricular delivery of VEGF in a rat model of ALS. *Nat Neurosci* **8**: 85–92.
- Tillo, M, Ruhrberg, C and Mackenzie, F (2012). Emerging roles for semaphorins and VEGFs in synaptogenesis and synaptic plasticity. *Cell Adh Migr* **6**: 541–546.

32. Coultas, L, Chawengsaksophak, K and Rossant, J (2005). Endothelial cells and VEGF in vascular development. *Nature* **438**: 937–945.
33. Shen, Q, Goderie, SK, Jin, L, Karanth, N, Sun, Y, Abramova, N *et al.* (2004). Endothelial cells stimulate self-renewal and expand neurogenesis of neural stem cells. *Science* **304**: 1338–1340.
34. Storkebaum, E, Ruiz de Almodovar, C, Meens, M, Zacchigna, S, Mazzone, M, Vanhoutte, G *et al.* (2010). Impaired autonomic regulation of resistance arteries in mice with low vascular endothelial growth factor or upon vascular endothelial growth factor trap delivery. *Circulation* **122**: 273–281.
35. Tufro, A, Teichman, J, Banu, N and Villegas, G (2007). Crosstalk between VEGF-A/VEGFR2 and GDNF/RET signaling pathways. *Biochem Biophys Res Commun* **358**: 410–416.
36. Yamamoto, M, Sobue, G, Yamamoto, K, Terao, S and Mitsuma, T (1996). Expression of mRNAs for neurotrophic factors (NGF, BDNF, NT-3, and GDNF) and their receptors (p75NGFR, trkA, trkB, and trkC) in the adult human peripheral nervous system and nonneural tissues. *Neurochem Res* **21**: 929–938.
37. Igarashi, Y, Utsumi, H, Chiba, H, Yamada-Sasamori, Y, Tobioka, H, Kamimura, Y *et al.* (1999). Glial cell line-derived neurotrophic factor induces barrier function of endothelial cells forming the blood-brain barrier. *Biochem Biophys Res Commun* **261**: 108–112.
38. Shah, JP, Phillips, TM, Danoff, JV and Gerber, LH (2005). An *in vivo* microanalytical technique for measuring the local biochemical milieu of human skeletal muscle. *J Appl Physiol* (1985) **99**: 1977–1984.
39. Cao, JP, Yu, JK, Li, C, Sun, Y, Yuan, HH, Wang, HJ *et al.* (2008). Integrin beta1 is involved in the signaling of glial cell line-derived neurotrophic factor. *J Comp Neurol* **509**: 203–210.
40. Lei, L, Liu, D, Huang, Y, Jovin, I, Shai, SY, Kyriakides, T *et al.* (2008). Endothelial expression of beta1 integrin is required for embryonic vascular patterning and postnatal vascular remodeling. *Mol Cell Biol* **28**: 794–802.
41. Blais, M, Levesque, P, Bellenfant, S and Berthod, F (2013). Nerve growth factor, brain-derived neurotrophic factor, neurotrophin-3 and glial-derived neurotrophic factor enhance angiogenesis in a tissue-engineered *in vitro* model. *Tissue Eng Part A* **19**: 1655–1654.
42. Verge, VM, Merlio, JP, Grondin, J, Ernfors, P, Persson, H, Riopelle, RJ *et al.* (1992). Colocalization of NGF binding sites, trk mRNA, and low-affinity NGF receptor mRNA in primary sensory neurons: responses to injury and infusion of NGF. *J Neurosci* **12**: 4011–4022.
43. Diamond, J, Coughlin, M, Macintyre, L, Holmes, M and Visheau, B (1987). Evidence that endogenous beta nerve growth factor is responsible for the collateral sprouting, but not the regeneration, of nociceptive axons in adult rats. *Proc Natl Acad Sci USA* **84**: 6596–6600.
44. Zwick, M, Teng, L, Mu, X, Springer, JE and Davis, BM (2001). Overexpression of GDNF induces and maintains hyperinnervation of muscle fibers and multiple end-plate formation. *Exp Neurol* **171**: 342–350.
45. Krakora, D, Mulcrone, P, Meyer, M, Lewis, C, Bernau, K, Gowing, G *et al.* (2013). Synergistic effects of GDNF and VEGF on lifespan and disease progression in a familial ALS rat model. *Mol Ther* **21**: 1602–1610.
46. Huang, YC, Kaigler, D, Rice, KG, Krebsbach, PH and Mooney, DJ (2005). Combined angiogenic and osteogenic factor delivery enhances bone marrow stromal cell-driven bone regeneration. *J Bone Miner Res* **20**: 848–857.
47. Paoni, NF, Peale, F, Wang, F, Errett-Baroncini, C, Steinmetz, H, Toy, K *et al.* (2002). Time course of skeletal muscle repair and gene expression following acute hind limb ischemia in mice. *Physiol Genomics* **11**: 263–272.